Techniques for designing prefabricated cable accessories based on hyperelastic material model

Techniques for Designing Prefabricated Cable Accessories Based on Hyperelastic Material Model

Yi Luo, Zhengyi Han, Xianzhang Lei, Mingyu Zhou, Hanyu Ye, Haitian Wang
Global Energy Interconnection Research Institute Europe GmbH
Markgrafenstr.34, 10117 Berlin Germany
Yanzhuo Liu
CYG Electric Co.,Ltd.
89 Jinfeng North Road, 519085, Zhuhai, China

***Abstract*- The interface between cable insulation and stress cone is commonly regarded as the most critical area of a pre-fabricated cable accessory. To enhance the overall performance, the contact pressure on the interface should be carefully designed. Linear material models are widely used in the industry to estimate the deformation of stress cone, but this method can hardly offer an accurate estimation for deformation above 5% because rubbers conform more to the non-linear material at this elongation range. This paper proposed a method, based on the hyperelastic model (Mooney-Rivlin) fitted from the uniaxial tensile test data. Compared to the present ones, this method offers a more accurate estimation of deformation above 10%, and therefore, helps in the verification of stress cone design and indirectly improves the reliability of high voltage cable accessories.**

I. INTRODUCTION

Ever since the introduction of high-voltage extruded cables, different types of cable accessories, including joints and terminations, have been implemented [1]–[3], among which, prefabricated cable accessories have been extensively applied nowadays, due to their accessibility of pre-testing and low-dependence on site condition.

The key part of prefabricated accessory is the stress cone, comprising insulation and electrode(s), which are made from insulating and semi-conductive rubber respectively. The stress cone is placed at the cutting edge of cable outer screen, as shown in **Error! Reference source not found.**. With an optimized geometry, the stress cone can unify the electric stress distribution in the internal insulation and therefore enhances the withstand voltage of the accessory.

The interface, referring to the red line in **Error! Reference source not found.**, is commonly reported as a critical spot [4]. A great amount of literature has reported that the tangential dielectric strength along the interface is highly dependent on the contact pressure [5]–[7], which needs to be within a reasonable range. On one hand, a low pressure cannot ensure a sufficient interface tangential dielectric strength; on the other hand, an excessively high contact pressure could possibly deform the cable insulation, while at high temperature, leading to a so-called bamboo phenomenon [8].

The contact pressure is acquired from the deformation of stress cone in case of one-piece accessory, as shown in Fig. 2. In order of a higher reliability, efforts have been made in finding the correlation between the pressure and the deformation. On the premise that the stress cone length did not change during deformation, P. Wang described the contact pressure with an analytic function of deformation [8]. In [9], X. Wang further calculated the displacement in both radial and axial direction, based on the finite element method. It is worth noticing that both methods above were based on linear material models, from which the rubber could act quite differently under an expansion of 15-30%.

This paper proposed a method, based on the hyperelastic model, for estimating the interface pressure and deformation of stress cone after installed. Compared to the commonly used one with a linear model, this method offers a more accurate estimation, and therefore, can help the engineer verify their design.

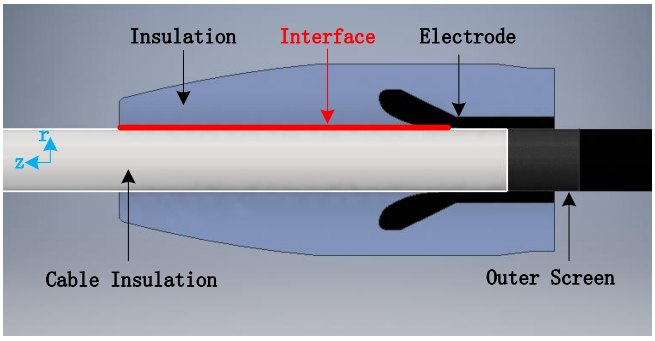

Fig. 1. Stress cone of a prefabricated cable termination

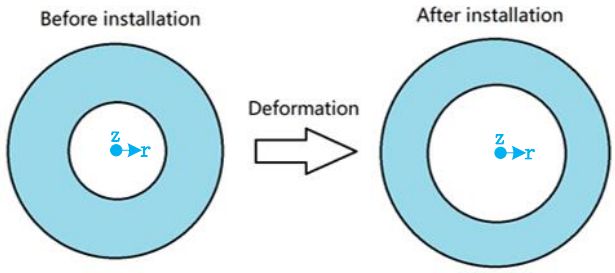

Fig. 2. Deformation of stress cone cross section before and after installation

II. HYPERELASTIC MODELS

The stress cone is often made of SIR (silicone rubber) or EPDM (ethylene propylene diene monomer rubber), either of which is non-linear elastic, isotropic, incompressible and strain rate independent, conforming closely to the ideal hyperelastic material. There are a number of hyperelastic material models, such as Neo

Hookean, Mooney-Rivlin, Arruda-Boyce, Yeoh, Ogden, etc., among which, Mooney-Rivlin model is often used to describe a stress-strain property of rubbers. Its two-parameter and five-parameter versions are as follows [10].

Mooney-Rivlin (two-parameter version):

$$P_2 = 2\cdot(1-La^{-3})\,(La \bullet C_{10}+C_{01}) \quad (1)$$

Mooney-Rivlin (five-parameter version):

$$P_5 = 2\cdot(1-La^{-3})\,[La\cdot C_{10}+2C_{20}\cdot La\cdot(I_1-3) + C_{11}\cdot La\cdot(I_2-3) + C_{01} + 2C_{02}(I_2-3) + C_{11}(I_1-3)] \quad (2)$$

where

$$I_1 = La^2+2/La \quad (3)$$

$$I_2 = 2\cdot La+1/La^2 \quad (4)$$

C_{10}, C_{01}, C_{11}, C_{20} and C_{02} are material parameters of the model; La represents the elongation rate, which is the ratio between stretched length L and original length L_0.

Fig. 3 introduces the stress-strain curve measured from a uniaxial tensile test of a type-1 piece of SIR, where the blue dots represent the measurement data. The slope of the curve at lower strain is significantly higher than those at higher ones, which makes linear curve fitting impossible to describe the extension behaviour accurately. This explains why the linear material elastic model is not suitable for this material.

Based on (1) and (2), the 2-parameter and 5-parameter Mooney-Rivlin models were fit with data in Fig. 3. It is clear to observe that 5-parameter Mooney-Rivlin model offers a better description of the stress-strain property than 2-parameter one.

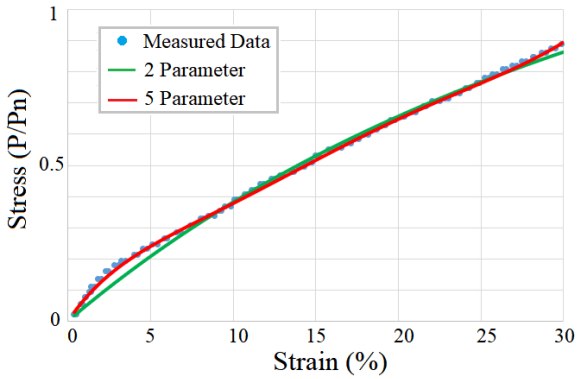

Fig. 3. Stress v.s. strain curve from a uniaxial tensile test of a Type-1 test piece. The green and red lines respectively represent the 2-parameter and 5- parameter Mooney-Rivlin models fit with the measured data.

III. ADVANTAGES OF SIMULATION METHOD

Without the aid of simulation software, only the outer dimension changes can be measured. Such as shortened length and increased outer diameter etc. However, the stretching of the inner material can't be measured. After the installation, the inner diameter of stress cone changes significantly greater than the outer diameter does. The material located near the inner surface of the stress cone is more stretched than the material located near the outer surface. The deformation offset of each point is not uniform. In this case, the production dimensions can only be approximately derived from the design dimensions. By using finite element simulation method this problem can be effectively solved. Fig. 4 shows the Mises equivalent stress diagram of a cross-section of a stress cone obtained by simulation. The tension of each point is visually displayed by using different colors, which makes the details very clear.

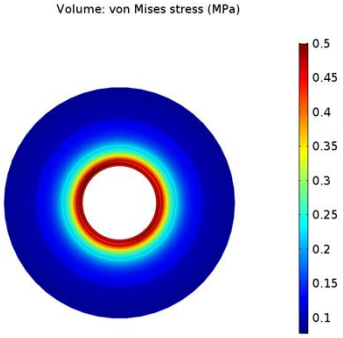

Fig. 4. Mises equivalent stress at one cross section of stress cone after installation

Through the simulation method, the displacement field in R and Z directions are shown in Fig. 5 and Fig. 6 respectively, in which the black lines indicate the original outline of stress. Since the model is of an axisymmetric structure, there is no component in the azimuth direction. Wherein, the displacement in R direction is the displacement of a certain point in the radial direction after stretching, and the offset in the Z-direction is the displacement of a certain point in the direction along the conductor after stretching. With the offsets in R and Z direction, the coordinates of a certain point before or after installation can be accurately derived from each other. After determining a sufficient number of key points, the stress cone production dimension can be determined. The offset is defined as the difference between the coordinates of design dimension and the coordinates of production dimension.

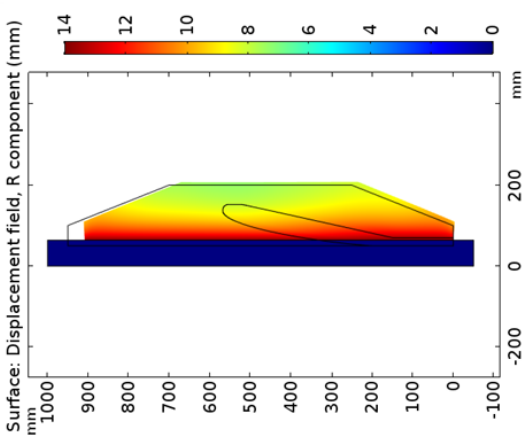

Fig. 5. R direction displacement

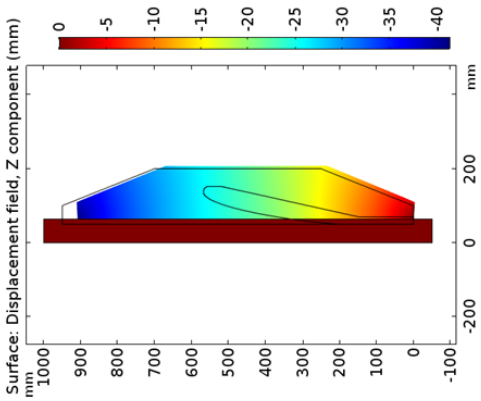

Fig. 6. Z-direction displacement

In addition, the simulation software such as Comsol can visually present the Mises equivalent stress, interface contact pressure and other results on demand (as shown in Fig. 7 and Fig. 8). The Mises equivalent stress diagram indicates that the tensile stress of the material in the stress cone is nonuniform. The material located near the inner surface of stress cone is clearly more stretched. The interface contact pressure is often high in the middle part and gradually reduced from middle to both ends. In addition, stress peaks also appear at both ends of the stress cone.

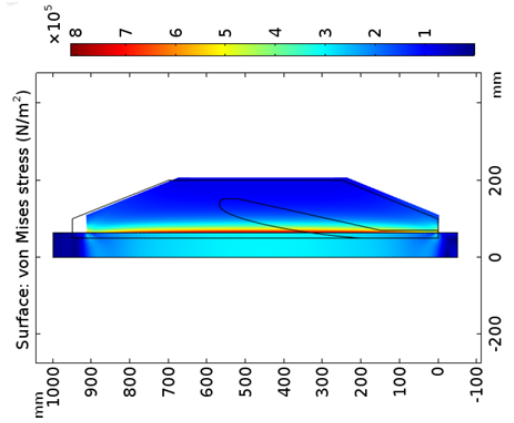

Fig. 7. Mises equivalent stress

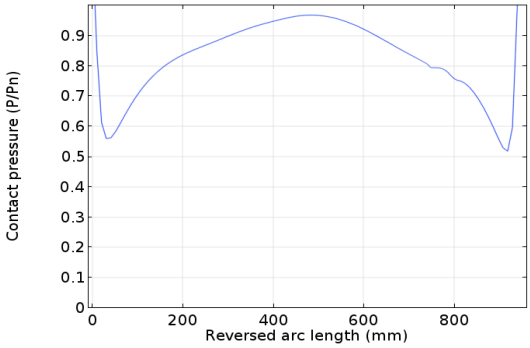

Fig. 8. Interface contact pressure

IV. FACTORS WHICH AFFECT CONTACT PRESSURE

A. Material properties

The material properties that affect the simulation results mainly refer to the stress-strain curve obtained in the tensile test of the material. In general, the more tensive the material (higher stress-strain curve), the higher the interface contact pressure. Liquid silicone rubber (LSR) is formed by mixed A compound and B compound through a curing process. The curing condition, such as temperature and duration, influence the mechanical properties of the material. Some manufacturers use a so-called post-cure method to further improve the mechanical properties of the products. By comparing the material tensile test data, it was found that the test data distributions of less cured specimens were relatively more dispersed. After post-cure, the data points are more concentrated, and the curve is higher which means better mechanical properties.

B. Stress Cone Shape

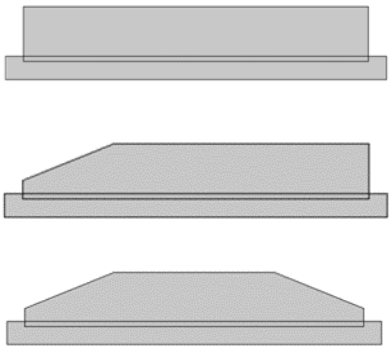

Fig. 9. Model of cylindrical, bullet and shuttle shape stress cone

For approximate calculation or simulation, the stress cone is usually simplified to a cylindrical shape with a uniform outer diameter. However, a true stress cone usually looks like a bullet with one narrow end or a shuttle with two narrow ends (as shown in Fig. 9). Usually, at the thicker area, the interface contact pressure is higher and at the thinner area, the pressure is lower. If the stress cone is simplified to a cylindrical shape, it will lead to deviation from the real situation, because it ignores the pressure drop due to the smaller outer diameter at the end of the stress cone. The following figure compares the interface contact pressure simulation results of three different stress cone shape, which is consistent with the theoretical analysis. The shape of deflector and stress cone should be optimized to ensure the hazardous area in the electrothermal coupling simulation is in a position with sufficient contact pressure and in the meantime the difficulty in installing the stress cone is reduced as much as possible.

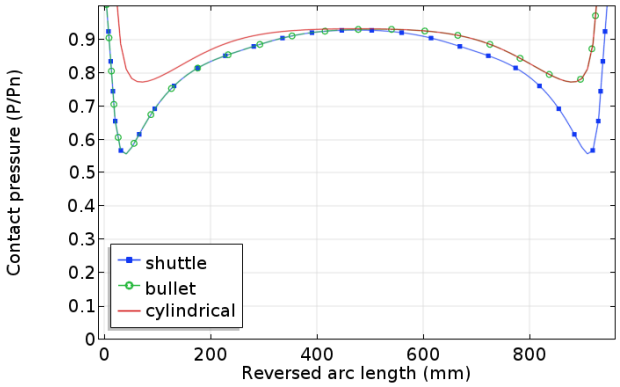

Fig. 10. Interface contact pressure of cylindrical, bullet and shuttle shape stress cone

C. *Mechanical Properties of Semi-Conductive Silicone Rubber Materials in Stress Cones*

If taking the semi-conductive part of the stress cone and the insulation part as a whole, it is easy to simulate using only the parameters of the insulation material. Using this simplification gets an accurate result only in the cases where the mechanical properties of the two materials are similar. This is usually not realistic. Fig. 11 compares the simulation results with and without the semiconducting details.

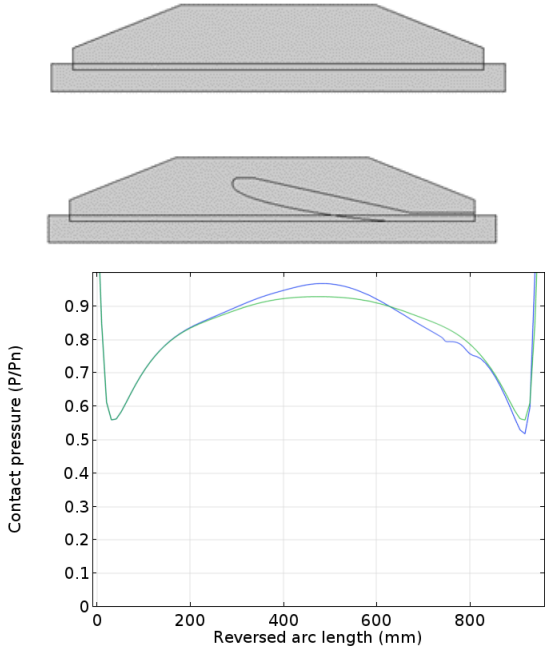

Fig. 11. Effect of semi-conductive part of stress cone interface contact pressure

The semi-conductive silicone rubber used in this case has a weaker tensile property than the insulating silicone rubber does. From the results, the semiconducting part does have some effect on the interface contact pressure at its height. The contact pressure at deflector corner has decreased. This location is also a critical area where electrical discharge can easily occur. Therefore, it is necessary to refine the simulation model so that the model was built as close as possible in details to the real product. The accuracy and the ability of detail analysis of the simulation method are the shortcomings of the traditional empirical formula method.

V. 2D Axis Symmetry Model vs. 3D Model

A. *Limitations of 2D Axis Symmetry Model*

Due to the structural characteristics of cables and accessories, the model built in the previous section uses only 2D axis symmetry model. Only half the cross-section is needed when modelling. One main advantage of this method is small computing amount so that the simulation runs fast. After comparison, the simulation results correspond well with the results of the normal 3D modelling. However, the 2D axis symmetry model also has its limitations. It can't be used to simulate non-axisymmetric cases.

B. *3D Model Cases*

Typical non-axisymmetric cases are cable insulation surface defects, cable eccentricity etc. The simulation for these cases can only be modelled directly with the 3D model. Fig. 13 shows a 3D simulation model of termination stress cone.

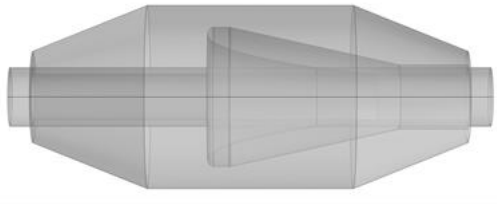

Fig. 12. 3D simulation model of termination stress cone simulation of surface defects of cable insulation with 3D model

If the surface of the cable insulation is improperly polished or scratched by hard objects after polishing, local dent may be observed. It can be verified through simulation that the interface contact pressure at the dent will decrease and the extent of the dent will be related to the depth and shape of the dent. In the hazardous area of the electrical test, dent should be straightly avoided.

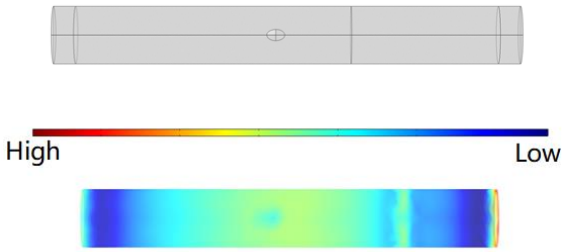

Fig. 13. Model of cable insulation surface dent (upper) and its interface contact pressure (lower)

VI. SUMMARY

In this paper, the method of calculating the interface contact pressure of the stress cone by using the finite element simulation is described. Compared with empirical formula, this method has the advantages of clear detail, high result accuracy, intuitionistic and rich content. The simulation model is built according to the actual size of the stress cone and cable. The material parameters are obtained by fitting data from the material tests. With proper boundary conditions, reasonable simulation results can be obtained. Mises equivalent stress, displacement before and after deformation and stress cone interface contact pressure can be visually displayed.

This paper presents a method to fit the hyperelastic material model parameters by using uniaxial tensile test data. Since Comsol has built in a number of commonly used hyperelastic material models, the fitting parameters can be directly used in the simulation model. Compared with the linear elastic material model, the hyperelastic material model can describe the behaviour of the silicone rubber more accurately.

In this paper, the influencing factors in the simulation of interface contact pressure are listed, such as the material properties, the shape of the stress cone and the details of the semiconducting part. The influence of these factors on the simulation results cannot be neglected.

In this paper, the 2D axis symmetry model and 3D model are compared. Several cases that can only be modelled with the 3D model have been mentioned. An example is given to show the simulation results of the interface contact pressure under the condition of local dent on the surface of cable insulation.

Two ±500kV DC terminations designed using the method described in this paper are undergoing type test (Fig. 14).

Fig. 14. ±500kV DC terminations under type test

ACKNOWLEDGMENT

This work was supported by the National Key Research and Development Program of China in its project entitle “Critical Technologies for Designing and Manufacturing ±500 kV DC Cables and their Accessories” (No. 2016YFB0900703); Science and Technology Project of SGCC (Research on Key Technologies for ± 500kV Direct Current Cable： Research on Key Technologies for the Preparation of DC Cable Accessories).

REFERENCES

[1] K. Ohata, H. Kojima, T. Shimomura, and K. Asahi, “Development of xlpe-moulded joint for high voltage xlpe insulated cable,” *IEEE Trans. Power Appar. Syst.*, vol. PAS-102, no. 7, pp. 1935–1941, 1983.

[2] Y. Nakanishi *et al.*, “Development of Prefabricated Joint for 275-kV XLPE Cable,” *IEEE Trans. Power Deliv.*, vol. 10, no. 3, pp. 1139–1147, 1995.

[3] Y. Ohki, “Extrusion-Molded Joints for World’s First Long-Distance XLPE Cable Line,” *IEEE Electr. Insul. Mag.*, vol. 7, no. 3, pp. 31–33, 1991.

[4] R. Ross, “Dealing with interface problems in polymer cable terminations,” *IEEE Electr. Insul. Mag.*, vol. 15, no. 4, pp. 5–9, 1999.
[5] T. Tanaka, M. Nagao, Y. Takahashi, A. Miyazaki, M. Okada, and Y. Yamashita, “Dielectric Characteristics of Interfaces in Prefabricated Joints of Extra-high Voltage XLPE Cables,” in *CIGRE*, 2000, pp. 1–8.
[6] D. Kunze, B. Parmigiani, R. Schroth, and E. Gockenbach, “Macroscopic internal interfaces in high voltage cable accessories,” in *CIGRE*, 2000, pp. 15–203.
[7] T. Klein, S. Zierhut, and E. Wendt, “Specific Requirements and Techniques for Designing Dry-Type Cable Terminations,” in *INMR*, 2017.
[8] P. Wang, J. Wang, Z. Li, J. Luo, and M. Xu, “Nonlinear Elastic Deformation of Cable Accessories during Expansion and Their Solutions,” *Electr. Wire Cable*, no. 6, pp. 1–3, 2016.
[9] X. Wang, C. Wang, K. Wu, D. Tu, S. Liu, and P. Jia, “An improved optimal design scheme for high voltage cable accessories,” *IEEE Trans. Dielectr. Electr. Insul.*, vol. 21, no. 1, pp. 5–15, 2014.
[10] C. Kumar, “Fitting Measured Data to Different Hyperelastic Material Models | COMSOL Blog,” *COMSOL BLOG*, 2015. [Online]. Available: https://www.comsol.de/blogs/fitting-measured-data-to-different-hyperelastic-material-models/. [Accessed: 29-Jan-2018].